

Frank Panton

Aasav Patel

Abstract—

I. INTRODUCTION

a) Background: : Robotic exploration has emerged as a crucial field, extending human capacity to rapidly and accurately search environments that are otherwise inaccessible or hazardous. By reducing the demand for human presence, robots like those used in patrolling applications can perform repetitive or dangerous tasks, thus conserving valuable human resources for more complex decision-making roles [1]. For instance, in agriculture, robotic systems can monitor crop health, detect pests, and distribute fertilizers efficiently, operating continuously over large areas [2]. These applications require the robot to deploy thorough search algorithms to ensure effective completion of the task. Additionally, robots are essential in reaching environments that are beyond human accessibility, such as deep underwater or radioactive sites, where they can collect data and perform tasks without risking human lives [3]. A clear example of this is in autonomous explosives detection, which requires significant accuracy of the sensors and robotic control systems [4]. Finally, robotic exploration can be used to expedite traditional human tasks, with the time-saving in some scenarios being life-saving, such as quickly navigating through debris to locate survivors in post-disaster search and rescue operations [5].

The Pololu 3PI+ robot [6] is particularly suited for experimental research in autonomous search due to its comprehensive sensor system and control capabilities. It is equipped with line sensors and bump sensors, which enable it to detect obstacles and variations in its terrain, with these sensors mirroring the practical use of a wide range of sensors seen in larger-scale robotic explorers, providing real-time data that enhance the robot's ability to make autonomous decisions. The integration of Arduino-compatible controllers and dual quadrature encoders facilitates precise movement and location tracking, crucial for maintaining accuracy in navigation throughout its task. This level of control and sensor integration in the 3pi+ makes it an excellent platform for developing and testing robotic search techniques that could be scaled up to larger, more complex systems.

b) Objective & Scope: The objective of this experiment is to deploy a PI+ robot in an unobserved area to locate and record the coordinates of waypoints. This will involve implementing different search strategies by adjusting the search algorithm type, the robot's speed, and the frequency of the search algorithm.

The project background highlighted the importance of thoroughness, accuracy, and speed in search robotics. These metrics will serve as key criteria for evaluating the effectiveness of various search algorithms, providing insights into their suitability of these algorithms in different scenarios.

c) Hypothesis: The following hypotheses suggest anticipated relationships between the varying search parameters and their impact on the measured search metrics, and will be investigated in this study.

- **H1:** More comprehensive algorithms are expected to identify a greater number of waypoints, resulting in a more thorough search of the space.
- **H2:** Conversely, as the search algorithms become more comprehensive, it is expected that search accuracy will decrease due to accrued kinematic error.
- **H3:** A faster search algorithm is hypothesized to decrease the location accuracy of identified waypoints.
- **H4:** Additionally, a faster search algorithm is anticipated to lead to a more efficient search strategy, resulting in finding more waypoints per unit time.

II. IMPLEMENTATION

The setup for implementing and testing the effectiveness of the search algorithm on the 3Pi+ robot involves defining either a square or sine wave search pattern, each with wavelengths of 200mm or 400mm. These patterns are illustrated in Fig. 1 which has been scaled to the size of an A3 sheet. The robot is programmed to follow these predetermined paths, with x and y coordinates detailed at a resolution of 200 points along each path. These coordinates are stored in a structure composed of x and y arrays. This resolution was chosen to balance detail and memory capacity, as higher resolutions would risk memory overflow.

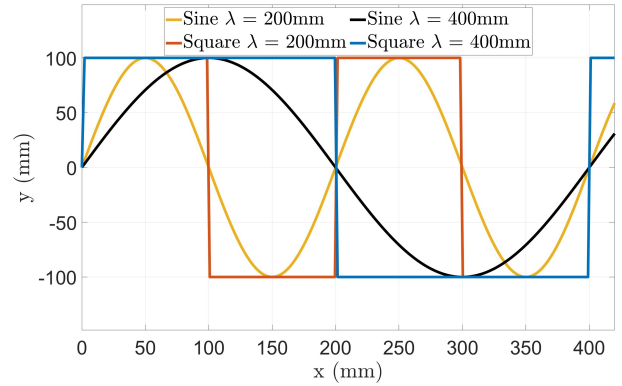


Fig. 1. Four different search algorithms that the robot will follow.

The robot navigates each coordinate using a finely tuned PID heading controller and its kinematic capabilities, which were developed in earlier stages of this project [?]. This implementation allows the robot to navigate smoothly and adjust its speed dynamically during the search process. When the robot approaches within 5mm of a search coordinate, a counter increments to track the coordinates found, and the robot proceeds to the next coordinate.

Concurrently, the robot's IR line sensors are actively scanning for waypoints. These waypoints, identified as black circles, trigger the sensors when passed over, indicating that their readings have surpassed a predetermined threshold. This prompts the robot to log its current position in an array of x and y values.

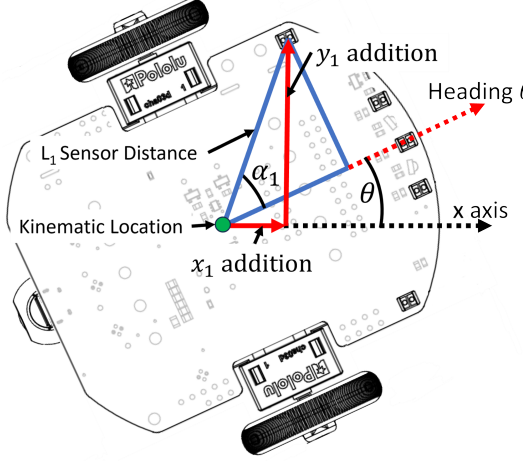


Fig. 2. Line sensor positions to accurately identify waypoint locations.

To enhance the accuracy of the waypoint coordinates, each sensor's position relative to the robot's center is calculated individually. This is because the kinematics of the robot provide the x and y position of the robot's center, not the actual position of the detecting sensor. The geometry involved is illustrated in Fig. 2, where α_1 represents the angle from the robot's center to the line sensor, L_1 is the distance from the robot's center to the sensor, and θ is the robot's orientation relative to the x-axis. The position adjustments for one the far left sensor shown in Fig. 2 can be computed as follows:

$$x \text{ addition} = x \text{ position} + L_1 \cos(\theta + \alpha_1) \quad (1)$$

$$y \text{ addition} = y \text{ position} + L_1 \sin(\theta + \alpha_1) \quad (2)$$

These calculations are applied to each sensor, with the caveat that angles for sensors on the right should be considered negative.

Upon completing the search algorithm, the robot stops and begins serially printing the locations of all detected waypoints. This allows for the data to be transferred to a laptop for further analysis and post-processing.

III. EXPERIMENT METHODOLOGY

a) Environment: The experimental environment consisted of two A3 sheets, each containing 10 different randomly generated waypoints represented by 15mm black circles. The exact x and y coordinates of these waypoints in the 2D search space were recorded. To ensure consistency and replicability, the starting location of the robot was marked on the A3 sheet, positioned at $(0, 0)$ as shown in Fig. 3. These sheets were securely taped down onto a white surface reducing the opportunity for slippage and the impact of the background on the sensors detecting false waypoints. Additionally, the environment's lighting was consistently purely artificial to minimise potential sensor interference.

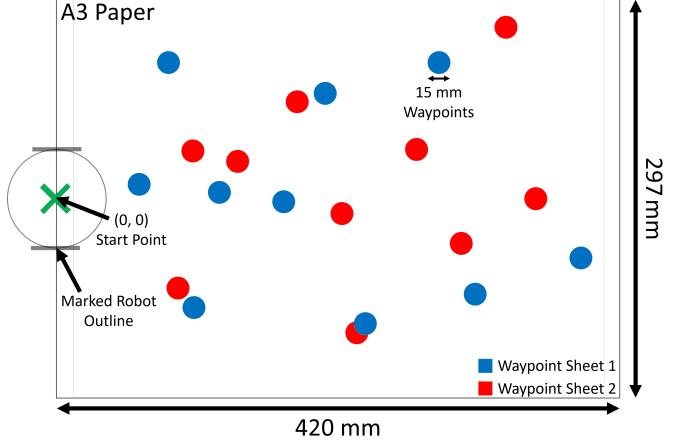


Fig. 3. Depiction of the two different environments and their 15mm waypoint distributions on an A3 sheet with the robot outlined at the start point for experimental consistency.

b) Controlled Variables: Throughout the experiment, several variables were carefully controlled to maintain consistency and ensure the reliability of the results. These controlled variables include:

- **Robotic Equipment:** The experiment utilised the same robot, a 3pi+. Additionally, the robot's battery was regularly monitored and maintained at a consistent level throughout the experiment to prevent fluctuations in performance due to battery depletion. This approach ensured uniformity in the robot's capabilities and behaviour across all trials.
- **Starting Position:** In each trial, the robot was placed at the same starting position on the A3 sheet. This controlled the initial conditions of the experiment and minimised variability in the starting location, enabling a fair comparison of the robot's performance across different runs.
- **Environmental Conditions:** Careful control was exercised over the experimental environment to minimise external influences on the robot's behaviour. Lighting conditions were kept constant, and the surface texture of the workspace remained consistent throughout the experiment. By maintaining a stable environment, any observed changes in the robot's performance could be attributed to variations in the independent variables rather than external factors.

This rigorous approach to controlling variables ensures that any observed differences in the dependent variables can be confidently attributed to changes in the independent variables rather than fluctuations in the experimental setup.

c) Independent Variables: In the experiment, the independent variables include the choice of the search algorithm, the search algorithm wavelength, λ , and the adjustments made to the robot's speed, offering a comprehensive exploration of search parameters.

- **Search Algorithm:** The robot's search algorithm is varied between a square wave and a sine wave pattern.
- **Robot Speed:** The speed of the robot is adjusted across three settings: slow, medium, and fast noted as speeds 1,

2, and 3 respectively in this experiment.

- **Wavelength/Frequency:** For each speed setting, the wavelength or frequency of the wave used in the search is also adjusted.

For each combination of the search algorithm, speed, and wavelength, the robot is run 25 times on each A3 sheet or search space as shown in Table I. This extensive testing protocol allows for robust analysis and ensures the reliability of the experimental results.

TABLE I

THE COMBINATIONS OF SEARCH ALGORITHM PARAMETERS AND THE NUMBER OF RUNS PER EXPERIMENT. THIS IS REPEATED FOR EACH A3 ENVIRONMENT RESULTING IN A TOTAL OF 600 RUNS COMPLETED.

Runs Per A3 Environment			Speed		
Wavelength	Square	200mm	1	2	3
		400mm	25	25	25
	Sine	200mm	25	25	25
		400mm	25	25	25

d) *Dependent Variables:* The chosen dependent variables are crucial indicators of the effectiveness and efficiency of the search algorithm:

- **Number of Waypoints Found:** This metric reflects the thoroughness of the search performed by the robot. It quantifies how many of the 10 random waypoints the search algorithm successfully locates. A higher number of waypoints found suggests a more comprehensive exploration of the search space.
- **Accuracy:** The accuracy metric evaluates how closely the measured location of each identified waypoint matches its exact location. The accuracy is calculated by summing the distances between the measured and exact locations of all waypoints found, divided by the total number of waypoints found. Therefore, higher accuracy corresponds to a lower ‘waypoint error value’ or a lower ‘distance to waypoint’. This average inaccuracy provides insight into the precision of the search algorithm. Additionally, assessing the accuracy of the first versus last waypoints found can help discern the impact of accrued error over time.
- **Time Taken (Speed of Search):** The time taken to complete the search pattern measures the efficiency of the search algorithm. It indicates how quickly the robot navigates through the search space to locate waypoints. A shorter time taken suggests a more efficient search algorithm, whereas a longer duration may indicate inefficiencies or challenges encountered during the search process.

e) *Procedure:* The experimental procedure involves configuring the desired combination of independent variables, including the choice of search algorithm, robot speed, and wavelength or frequency. The robot is then positioned at the starting location on the A3 sheet, ensuring consistency across runs. After resetting the robot, the search algorithm is initiated, and the robot autonomously navigates through the search space to locate the waypoints. Upon completion of the run, the locations of the waypoints found and the time taken to complete

the search are recorded and transferred to an Excel sheet for further analysis. This process is repeated for a total of 25 runs with the current setup, ensuring a sufficient sample size for statistical analysis. Subsequently, the experimental variables are systematically adjusted to the next setup configuration, and the procedure is repeated. Finally, the collected data is analysed to evaluate the impact of varying search parameters on the number of waypoints found, accuracy, and time taken to complete the search. Through this systematic approach, the performance of different search algorithms and parameter configurations can be evaluated comprehensively.

To consider: - mentioning how we remove anomalous

IV. RESULTS

a) *Relationship Between Search Algorithm Combination and Thoroughness of Search:* The effectiveness of different search algorithms in identifying waypoints has been evaluated using box and whisker plots, aggregating data across two separate A3 search environments as shown in Fig. 4. The results indicate that search patterns with shorter wavelengths and frequent turns typically yield a higher number of waypoints. Specifically, the shorter wavelength configurations for both square and sine wave patterns have higher median values, with square wave patterns achieving a median of 7 waypoints and sine wave patterns achieving 6.6 waypoints, both exceeding the overall average of 5.5 waypoints. Conversely, the 400mm wavelength searches both share a median of 4 waypoints found which is below the average indicating a less thorough search.

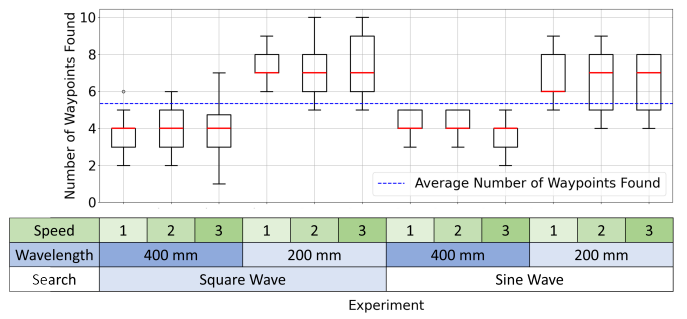


Fig. 4. Number of waypoints found for each search parameter combination in both A3 environments.

Although both the square and sine wave patterns perform similarly under identical speed and wavelength conditions—demonstrated by comparable medians and similar distributions of data within the upper and lower quartiles—there is a trend in the difference in the maximum values achieved. The maximum value for all square wave searches is higher or the same as the corresponding sine wave searches. This suggests that square wave patterns may have the potential to find more waypoints under certain conditions.

b) *Relationship Between Accuracy and Search Algorithm Combination:* To evaluate the positional accuracy of each search algorithm, the average distance error between the measured and exact waypoint locations was calculated and visualised using box and whisker plots for each search algorithm as shown in Fig. 5. A blue line across the plots indicates

the mean distance error for all algorithms, with lower values indicating higher accuracy.

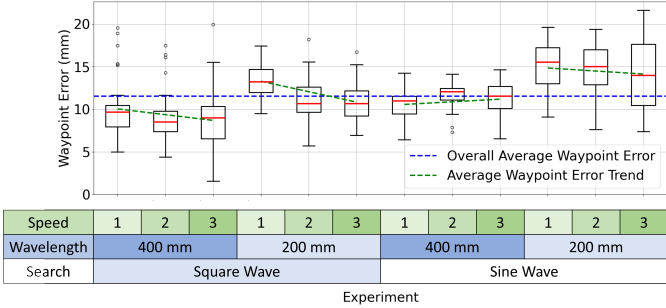


Fig. 5. Accuracy of each search parameter combination shown by distance between waypoint position and robot recorded waypoint position in both A3 environments.

The square wave outperforms the sine wave in terms of accuracy. For example, the 400mm wavelength square wave search shows an average error of 9mm across all speeds, which is x% more accurate than the overall mean, while the 400mm wavelength sine wave search averages an 11.5mm error, aligning exactly with the mean. Similarly, the 200mm wavelength searches reveal that the square wave maintains an error rate close to the mean, whereas the sine wave search demonstrates a noticeable increase in error, suggesting that the sine wave pattern may accumulate more kinematic errors.

Additionally, this data reveals search algorithms with shorter wavelengths, which necessitate more frequent turns, tend to have higher error rates. The 200mm wavelength square wave searches exhibit an x% decrease in accuracy compared to the 400mm square wave searches. This trend is mirrored in the sine wave searches, where the 200mm searches also show an x% increase in error compared to their 400mm counterparts.

A final observed trend is that faster search speeds generally lead to greater accuracy. This is evident in both the 200mm and 400mm wavelength searches for square waves and the 200m sine wave searches, where there is an x%, x% and x% increase in accuracy from the slowest speed to the fastest speed respectively. However, the 400mm sine wave searches do not conform to this trend, as the variation in accuracy from the fastest to the slowest speed is minimal, suggesting that this trend may not apply to certain algorithm configurations.

To investigate the accumulation of kinematic errors, the average errors of the first and last waypoints were analysed and are illustrated in Fig. 6. The data consistently show that the error for the first waypoint (red line) is significantly lower than that for the last waypoint (blue line), suggesting that kinematic error accumulates throughout the run. Notably, the errors for the slow 400mm sine wave pattern are closer together compared to other configurations. This is attributed to the fact that the lower frequency sine wave tends not to detect an early waypoint, resulting in a shorter interval to accrue errors between the first and last waypoints.

Moreover, the data revealed a distinct pattern where greater errors are observed at the last waypoint for search algorithms with shorter wavelengths. For example, the 200mm wavelength square wave search shows an average error of 17mm

at the last waypoint, whereas the 400mm wavelength square wave search exhibits a lower average error of 11.5mm. A similar increase in error at the last waypoint with decreasing wavelength is observed in the sine wave patterns. The heightened error in short wavelength searches likely stems from the increased number of turns and the greater distance covered, which heightens the potential for kinematic errors such as wheel slippage and rounding inaccuracies.

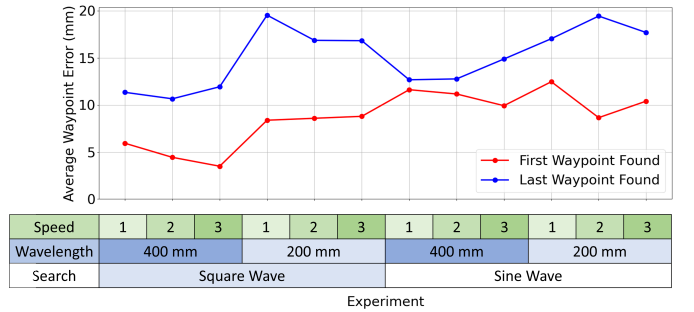


Fig. 6. Comparison of the average error of each search algorithm combination, between its first waypoint found and its last waypoint. Showing error in waypoint accuracy increases throughout the run

c) The Relationship Between Search Algorithm Combination and Efficiency of Search: To investigate the speed and efficiency of various search strategies, the time taken per waypoint was plotted for each type of search, as shown in Fig. 7. A key observation from this graph is that increasing the speed setting consistently reduces the time taken per waypoint, indicated by the downward green trend lines. For instance, at the highest speed setting, the time taken per waypoint is faster by x seconds for the 400mm square wave, x seconds for the 200mm square wave, x seconds for the 400mm sine wave, and x seconds for the 200mm sine wave.

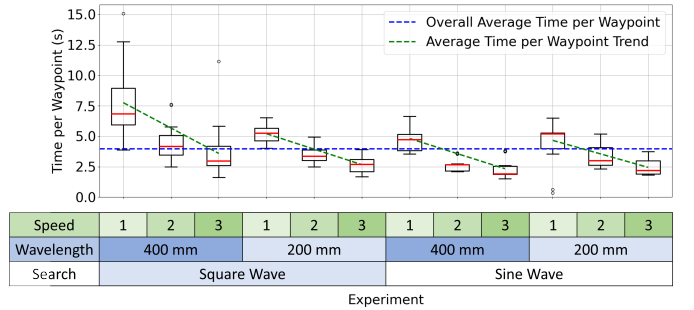


Fig. 7. This shows the average time taken for a search parameter combination to find a waypoint.

This finding is supported by data from Fig. 4, which shows minimal variation in the number of waypoints found across different speeds for the same search paths. This suggests that higher speeds do not compromise the effectiveness of waypoint detection or cause significant deviations from the target path. Therefore, using higher speeds across the same wavelengths and search types is more efficient. (add limitation of this as there will be an upper limit to this contained by either the robot or the difficulty to pid tune the search pattern for that speed.)

Moreover, the sine wave search strategy is more efficient than the square wave. The average time per waypoint for the sine wave at 400mm and 200mm wavelengths is **3.6 seconds** and **3.4 seconds**, respectively, compared to **6 seconds** and **4 seconds** for the square wave at the same wavelengths. This efficiency likely stems from the sine wave's continuous turning pattern, in contrast to the square wave's sharp 90-degree turns, which can cause overshoots from the PID heading control. Such overshoots slow down the robot as it corrects its course, thus increasing the time per waypoint. This is particularly evident in the slow square wave search at the larger wavelength, which not only performs a less thorough search but also travels slowly, especially around corners. Anomalies represented by circles above the 400mm wavelength square wave patterns could be due to significant PID overshoots during turns, requiring time for the integral gain of the PID to realign the heading before proceeding.

V. DISCUSSION

H1: *More comprehensive algorithms are expected to identify a greater number of waypoints, resulting in a more thorough search of the space.*

The results supported this hypothesis, as shown in Fig. 4. Algorithms with shorter wavelengths, which involve more frequent turns and detailed coverage, consistently identified a greater number of waypoints. This trend confirms the hypothesis's utility in predicting the outcomes of intricate search patterns and has helped guide this investigation, by revealing the relationship between algorithm complexity and search thoroughness.

However, it is expected that this relationship may have limitations at extremely short wavelengths where the search algorithm might identify all possible waypoints. Beyond this point, further reductions in wavelength and increases in thoroughness might not lead to improvements in search outcomes but could instead increase the inefficiency of the search as the robot may begin to retrace areas it has already covered. This potential inefficiency was not reached in this investigation but represents an obvious next step for future research to detail the limits of this relationship.

H2: *It is hypothesised that as search algorithms become more comprehensive, search accuracy will decrease due to increased kinematic error.*

Evidence from Fig. 5 supports the hypothesis that a more comprehensive search, characterised by shorter wavelengths, results in higher errors. This increase in error can be attributed to kinematic errors that accumulate from frequent turning movements. To substantiate this, an analysis of the errors at the first and last waypoints for various search patterns was conducted (Fig. 6). The results revealed significantly higher errors at the last waypoints compared to the first across all search combinations, suggesting a buildup of error over time.

A plausible explanation for this accumulated error is the limitations of the robot's PID control, particularly during frequent turns. The sine wave algorithms, which require more turns and less straight-line travel compared to their square wave counterparts, generally exhibited higher errors. These

algorithms cause the robot to engage in a 'jerky' motion, frequently stopping to correct its course. This can lead to wheel slippage and increased rounding errors at each stop, which increase the error in the kinematics especially when the robot is not gaining any distance or caught between encoder counts.

To address this issue, a staged PID control system was implemented to adjust the proportional and integral gains for the robot's heading controller; sharper gains for turns and moderated gains for straight-line travel. While this approach visually improved performance in the square wave pattern—where turns are consistent at close to 90° angles—the sine wave pattern still displayed more frequent jerks, particularly during moments of continuous turning. Improving control and minimising stop-start motion through the incorporation of a better heading PID such as a fuzzy logic PID, known for its efficacy in DC motor control, could be beneficial [7].

H3: *A faster search algorithm is hypothesized to decrease the location accuracy of identified waypoints.*

Contrary to expectations, experimental results from Fig. 5 revealed that increasing the speed of the search algorithm improved accuracy, rather than causing the anticipated increase in wheel slippage and decreased accuracy. This could mean that the speeds tested did not reach the levels at which kinematic or control issues typically occur. To better understand the impact of speed on accuracy, additional experiments at even higher speeds would be necessary.

Additionally, the relationship between the robot's speed and its accuracy is more complex than anticipated. Initially, it was thought that wheel slippage from increased speed would be the main source of error. However, it appears that speed more significantly affects PID control, which in turn has a greater impact on accuracy. At lower speeds, the robot struggles with sharp turns, often overshooting and abruptly stopping to correct its course. This behaviour, especially noticeable during 90° turns, likely causes kinematic errors and leads to inaccuracies.

Despite the introduction of a staged PID to enhance control during turns, the robot failed to consistently perform smooth manoeuvres at lower speeds. In contrast, at higher speeds, the robot operated more smoothly, possibly due to its ability to more effectively overcome frictional forces and inertial loads, thus maintaining better kinematic accuracy. These observations show the complexity of the interplay between speed, accuracy, and control in robotic search algorithms. This hypothesis, similar to Hypothesis 2 (H2), suggests that refining PID control is essential to fully understand the effects of increasing speed.

H4: *Additionally, a faster search algorithm is anticipated to lead to a more efficient search strategy, resulting in finding more waypoints per unit time.*

The data robustly supported this hypothesis, as faster speeds consistently resulted in more efficient searches with reduced times per waypoint across different algorithmic settings, as shown in Figure 7. This finding validates the hypothesis and underscores its effectiveness in predicting the benefits of increased speed within robotic search algorithms.

The hypotheses have clearly demonstrated the complex relationship between speed, accuracy, and thoroughness in robotic search strategies. Hypothesis 3 (H3) explored how increased speed might decrease accuracy, while Hypothesis 4 (H4) showed that higher speeds enhance thoroughness by enabling faster waypoint detection. This reveals a delicate balance between the impacts of speed on both thoroughness and accuracy, highlighting an inherent connection between these two aspects.

This relationship is visually captured in Fig. 8, which illustrates the interaction between thoroughness (measured by the number of waypoints detected) and accuracy (indicated by the average error in a search strategy). The data show distinct patterns: more thorough searches typically use shorter wavelengths, which provide more frequent and detailed coverage. In contrast, longer wavelengths, especially square waves at high speeds as noted in Hypothesis 2 (H2), are more effective for optimizing accuracy. This indicates a clear trade-off between thoroughness and accuracy, largely dictated by wavelength.

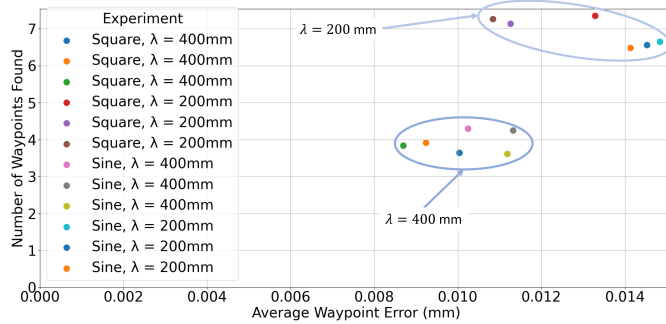


Fig. 8. Number of waypoints found against waypoint error, showing distinct clusters based on the search path wavelength.

These findings emphasise the importance of strategic decision-making in the design and implementation of robotic search algorithms. Whether the priority is maximising coverage (thoroughness) or ensuring precise navigation (accuracy), the selection of wavelength and speed parameters is critical. This refined understanding enables a more focused deployment of robotic systems for specific tasks, ensuring that operational priorities guide the technological application.

VI. CONCLUSION AND FURTHER WORK

using the insights and relationship gained from the investigation, the optimal search parameters when prioritising different metrics of search have been established in table X:

TABLE II
OPTIMAL SEARCH PARAMETERS FOR THOROUGHNESS, ACCURACY AND TIME PER WAYPOINT

Metric	Optimal Search Parameters		
Metric	Wavelength	Speed	Search Pattern
Thoroughness	200 mm	3	Square/Sine
Accuracy	400 mm	3	Square
Time per Waypoint	200 mm	3	Sine

For this robot, more thorough searches are achieved with shorter wavelengths at higher speeds resulting in more way-

points being found. These settings allow the robot to cover more ground and detect waypoints or objects with higher frequency. These insights can be extrapolated to real-world applications where thorough coverage is critical. For example, in environmental monitoring, robots need to systematically survey habitats or ecosystems, ensuring comprehensive data collection across diverse and extensive areas. The wavelength parameter would need to be adjusted based on the range of the robot's sensors, to ensure it is small enough to maintain thoroughness of search but not cause overlapping of previously explored areas.

that involve frequent turns and detailed coverage.

REFERENCES

- [1] N. Basilico, "Recent trends in robotic patrolling," *Current Robotics Reports*, vol. 3, 06 2022.
- [2] S. Fountas, N. Mylonas, I. Malouñas, E. Rodias, C. Hellmann Santos, and E. Pekkeriet, "Agricultural robotics for field operations," *Sensors*, vol. 20, no. 9, 2020. [Online]. Available: <https://www.mdpi.com/1424-8220/20/9/2672>
- [3] J. Huo, M. Liu, K. Neusyipin, H. Liu, M. Guo, and Y. Xiao, "Autonomous search of radioactive sources through mobile robots," *Sensors*, vol. 20, p. 3461, 06 2020.
- [4] G. Fedorenko, H. Fesenko, V. Kharchenko, I. Kliushnikov, and I. Tolkunov, "Robotic-biological systems for detection and identification of explosive ordnance: concept, general structure, and models," *Radio-electronic and Computer Systems*, pp. 143–159, 05 2023.
- [5] A. Din, M. Jabeen, K. Zia, A. Khalid, and D. K. Saini, "Behavior-based swarm robotic search and rescue using fuzzy controller," *Computers & Electrical Engineering*, vol. 70, pp. 53–65, 2018. [Online]. Available: <https://www.sciencedirect.com/science/article/pii/S0045790618314216>
- [6] Pololu-Corporation, *Pololu 3pi+ 32U4 User's Guide*, 2022.
- [7] D. Somwanshi, M. Bundele, G. Kumar, and G. Parashar, "Comparison of fuzzy-pid and pid controller for speed control of dc motor using labview," *Procedia Computer Science*, vol. 152, pp. 252–260, 2019, international Conference on Pervasive Computing Advances and Applications- PerCAA 2019. [Online]. Available: <https://www.sciencedirect.com/science/article/pii/S1877050919306702>